Journal of Biomechanics 47 (2014) 367–372

Contents lists available at ScienceDirect

Journal of Biomechanics

journal homepage: www.elsevier.com/locate/jbiomech
www.JBiomech.com

The effect of hydration on mechanical anisotropy, topography and fibril organization of the osteonal lamellae

A. Faingold [a], S.R. Cohen [b], R. Shahar [c], S. Weiner [d], L. Rapoport [e], H.D. Wagner [a,*]

[a] Department of Materials and Interfaces, Weizmann Institute of Science, Rehovot 76100, Israel
[b] Chemical Research Support, Weizmann Institute of Science, Rehovot 76100, Israel
[c] Koret School of Veterinary Medicine, The Hebrew University of Jerusalem, Rehovot 76100, Israel
[d] Department of Structural Biology, Weizmann Institute of Science, Rehovot 76100, Israel
[e] Department of Science, Holon Institute of Technology, Holon 58102, Israel

ARTICLE INFO

Article history:
Accepted 18 November 2013

Keywords:
Osteon
Dehydration
Modulus
Anisotropy
Lamellation

ABSTRACT

The effect of hydration on the mechanical properties of osteonal bone, in directions parallel and perpendicular to the bone axis, was studied on three length scales: (i) the mineralized fibril level (~100 nm), (ii) the lamellar level (~6 μm); and (iii) the osteon level (up to ~30 μm).We used a number of techniques, namely atomic force microscopy (AFM), nanoindentation and microindentation. The mechanical properties (stiffness, modulus and/or hardness) have been studied under dry and wet conditions. On all three length scales the mechanical properties under dry conditions were found to be higher by 30–50% compared to wet conditions. Also the mechanical anisotropy, represented by the ratio between the properties in directions parallel and perpendicular to the osteon axis (anisotropy ratio, designated here by AnR), surprisingly decreased somewhat upon hydration. AFM imaging of osteonal lamellae revealed a disappearance of the distinctive lamellar structure under wet conditions. Altogether, these results suggest that a change in mineralized fibril orientation takes place upon hydration.

1. Introduction

The major constituents of bone are mineralized collagen fibrils and water (Weiner and Wagner, 1998). Cortical bone contains about 20 vol% of water (Techawiboonwong et al., 2008) which varies inversely with the mineral content: during the mineralization process, the collagen volume fraction remains constant and the mineral replaces the water (Weiner and Wagner, 1998). With age, the mineral content in bone increases, resulting in diminished water content. Hence, understanding how water content affects mechanical properties and structure of bone is important in view of bone age-related behavior. The water in bone can be bound to the organic matrix and crystal surfaces (Techawiboonwong et al., 2008), and can be present as bulk water that fills pores, canaliculi and the vascular system (Turov et al., 2006). Nomura et al. (1977) identified four types of water: two nonfreezable, corresponding to the structural and bound water, and two freezable, corresponding to the unbound bulk water. Moreover, recent studies suggest that the amount of water varies between the different lamellar sublayers (Reznikov et al., 2012; Utku et al., 2008), raising new questions about the role of water on local structure and properties. Structurally, recent studies suggest (Reznikov et al., 2012) that fibrils have denser mineralized packing in dry samples than in high pressure frozen samples, however, their orientation and organization remains similar. Utku et al. (2008) measured the shrinkage of osteonal lamellae in different directions, comparing environmental SEM images under 100% humidity and dry conditions. They found a contraction of 1.2% perpendicular to the lamellae but no contraction parallel the lamellae, in longitudinal sections. In a transversal plane the contraction in all directions was reported to be the same.

In addition to structural effects, water plays an important role in terms of mechanical properties. Young's modulus (E) is lower by 30–50% in hydrated bone samples compared to the dehydrated ones (Feng et al., 2012; Guidoni et al., 2010; Rho and Pharr, 1999), where dehydration means drying in air for at least 24 h. Another interesting question is whether the mechanical effect of water is isotropic or not. Osteonal bone is mechanically anisotropic on several length scales (Fan et al., 2002; Liu et al., 2000; Reilly and Burstein, 1975; Riches et al., 1997; Ziv et al., 1996).The bone anisotropy ratio (AnR), defined as the ratio of Young's moduli in directions parallel and perpendicular to the bone axis, respectively, is larger than 1. However, comparing dry and wet conditions, it is still not clear whether the anisotropy ratio is conserved. Guidoni et al. (2010) reported similar changes in E in two perpendicular directions in osteonal bone at the lamellar length scale, namely,

* Corresponding author. Tel.: +972 8 934 2594; fax: +972 8 934 4137.
E-mail address: daniel.wagner@weizmann.ac.il (H.D. Wagner).

0021-9290/$ - see front matter © 2013 Elsevier Ltd. All rights reserved.
http://dx.doi.org/10.1016/j.jbiomech.2013.11.022

the anisotropy ratio remained constant upon dehydration. On the other hand, Wolfram et al. (2010) and Spiesz et al. (2012) reported an anisotropic change in E on rehydration, in trabecular lamellar bone (at length scale $>10\ \mu m$) and mineralized tendons (at length scale $>5\ \mu m$), respectively. Both of them reported an increase of AnR under wet conditions compared to dry ones. Likewise, Seto et al. (2008) reported a drastic decrease in AnR upon drying of parallel fiber bone, at length scale of $5\ \mu m$. Notice, that both mineralized tendons and parallel fibered bone have a structure of parallel mineralized collagen fibrils. Thus, although the results reported by Spiesz et al. (2012) and Seto et al. (2008) are at the micro-scale, they would represent a nano-scale organization at the osteonal bone. The question of how the water affects mechanical anisotropy in osteonal lamellae therefore remains open.

Here, we investigate the effect of unbound water on the mechanical properties and structure of osteonal lamellar bone on three length scales, from the mineralized fibril level up to the osteonal level, using atomic force microscopy, nanoindentation and microindentation.

2. Experimental

Samples from a frozen metacarpal bone of a 5 year old male horse were studied. All samples were cut using a Minitom cutting instrument (Struers) under constant watering and polished according to a procedure described in our previous work (Faingold et al., 2012). Sample sizes varied from about 5 mm $\times$ 5 mm $\times$ 5 mm for micro- and nano- indentations to 10 mm $\times$ 5 mm $\times$ 1 mm for AFM measurements. After polishing, samples were kept under ambient conditions for at least 24 h. Afterwards, no dependence of the measured properties on time was observed and these are samples referred to as studied under "dry" conditions. The "wet" samples were measured after incubation under phosphate buffered saline (PBS) for at least 12 h for the micro- and nano-indentation, and for 1 h under de-ionized water for the AFM measurements. To check the water content of "dry" samples, seven specimens from the studied bone were dried in an oven at 100 °C for 4 h, to remove the unbound water (Cohen et al., 2012). The specimens were weighed before and immediately after the drying, showing a loss of $9\pm1\%$ of weight, indicating that the specimens measured under "dry" conditions in fact contained about 9 wt% water. The same samples were kept in PBS solution for at least 12 h, to check water content under "wet" conditions. The "wet" samples contained up to 12 wt% water, when measured in the same way. Thus, actually the "dry" or "dehydrated" samples, as they are referred to in the literature (Feng et al., 2012; Guidoni et al., 2010; Rho and Pharr, 1999), still contain about 75% of the unbound water.

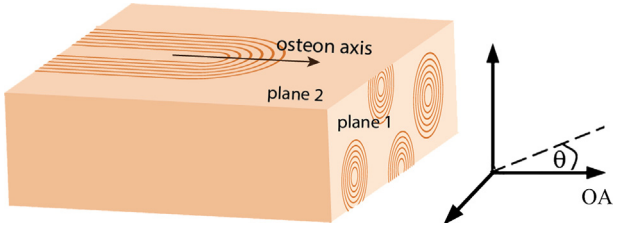

Fig. 1. Schematic illustration of osteonal bone sample. The measurement directions (normal to the surface) of plane 1 and plane 2 are parallel and perpendicular to the to the osteon axis (OA), respectively.

Samples with two orientations were prepared: parallel and perpendicular to the bone axis, the latter being approximately the osteon axis (OA). All mechanical measurements used in this work measure the properties in the direction normal to the surface. The angle between the osteon axis and the direction of measurements is represented by θ (Fig. 1). Thus, when a surface perpendicular to the osteon axis is measured (plane 1, see Fig. 1), the resultant mechanical property corresponds to the direction parallel to the osteon axis ($\theta=0^\circ$, see Fig. 1). Similarly, measurements of plane 2 correspond to the direction perpendicular to the osteon axis, $\theta=90^\circ$ (Fig. 1).

2.1. Atomic force microscopy

Flat samples, about 10 mm $\times$ 5 mm $\times$ 1 mm, were ground and polished according to the procedure described in our previous work, as detailed above (Faingold et al., 2012). After the AFM dry measurements, the sample was immersed in situ in de-ionized water for at least 60 min and then tested inside the AFM fluid cell at the same location. Longer exposure to water yielded no further change in the measured properties. These measurements were performed under de-ionized water rather than PBS, because for measurements in PBS using AFM an additional long-range force was present, presumed due to electrostatics. Two to three osteons were studied in each plane, under every set of conditions.

The topography and Young's modulus were mapped simultaneously using Peak Force Quantitative Nanomechanical Property Mapping PF-QNM (Bruker multimode AFM with Nanoscope V electronics). Either a diamond tip glued to sapphire cantilever with spring constant of 290 N/m (Microstartech), or an integrated silicon cantilever with nominal stiffness of 200 N/m (Bruker TAP525), were used, so as to be sensitive to the surface compliance of bone. For this scanning technique, the depth of probe penetration was about 10 nm, avoiding plastic deformation which could be observed in topography images as slight depression over the region scanned. Using this technique, the software automatically calculates Young's modulus, according to the DMT method (Derjaguin et al., 1975). The E values of samples, thus, obtained under wet conditions were in range of 1–3 GPa only, similar to those expected for non-mineralized collagen fibrils (Weiner and Wagner, 1998). However, analysis of individual force curves revealed that the fit to the DMT model was quite poor. The force curves also did not fit common elastic schemes, such as the Herzian model for spehrical indenter or Sneddon's model for a conical punch. This was due to a very gradual appearance of a repulsive force at relatively large distance from the contact surface (see Fig. 2b). Although modulus values in this range have been previously reported by Balooch et al. (2008), we suspect there may be a thin surface layer of demineralized fibrils which control the early part of the force–displacement curve so that these values do not represent the mineralized fibril properties. Due to the difficulties in fitting the data to a standard model, a simpler analysis was chosen to compare the wet and dry samples, as follows. Stiffness of the sample is a direct experimental observable – it is simply the slope of force–displacement curves acquired during AFM measurements. With knowledge of the contact area dependence on depth, stiffness is used to calculate E. Here, the stiffness over a fixed part of the unloading curve (i.e., at a given sample deformation) was used to compare the wet and dry samples. Quasistatic indentations of 120–140 nm depth, chosen to achieve a clear linear segment in curve, were performed using the silicon cantilever with nominal stiffness of 200 N/m, under both dry and wet conditions. At least 100 indentations, representing 2–3 osteons, were performed in each plane, and under every set of conditions. The average specimen stiffness was calculated for depths between of 90% and 65% of the maximum on the unloading curve (where it is less likely to be affected by the surface forces). Stiffness under wet and dry conditions, of both planes 1 and 2 were measured.

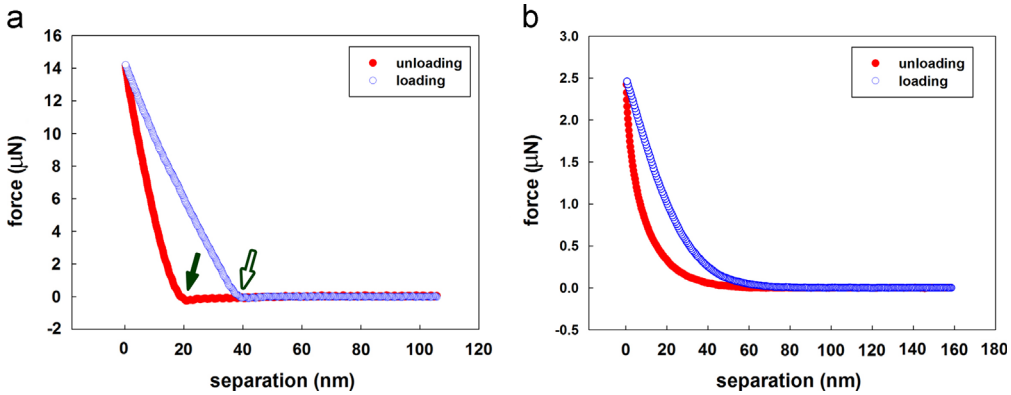

Fig. 2. AFM force curves for samples under (a) dry and (b) wet conditions showing the change in force as a function of probe-surface separation. Under dry conditions (a) there is a clear point of contact, for both loading and unloading, marked by hollow and full arrows, respectively. Under wet conditions (b) the force rises very gradually as a function of distance and no clear point of contact may be distinguished.